24 - 25 May 2018, Brussels, Belgium

Voltage Unbalance Mitigation by Using the Three-phase Damping Control Strategy in Active Rectification Mode

Dimitar V. Bozalakov, Mohannad Jabbar Mnati, Alex Van den Bossche, Lieven Vandevelde
Department of Electrical Energy, Metals, Mechanical Constructions and Systems, EELAB Ghent University, Ghent, Belgium
Email: dibozala.bozalakov@UGent.be

***Abstract*—The constantly increasing interest towards the electric and plug-in hybrid electric vehicles will increase the voltage unbalance and overvoltages in the distribution grids and therefore, the power quality of the grid voltage might be put in a danger. To overcome this issue more sophisticated control strategies for the battery chargers must be used that are able to improve the power quality in the low voltage grid. In this paper, a solution based on the three-phase damping control strategy is proposed that can be used to control the power electronic rectifiers in the battery chargers such that asymmetrical phase currents are drawn and thus the voltage unbalance at the point of common coupling is mitigated.**

***Index Terms*—Voltage unbalance mitigation, overvoltages, power factor corrector, electric vehicles, damping control strategy**

I. Introduction

Nowadays, the use of electric vehicles (EV) is continuously growing as a solution for reducing the greenhouse gases. The EV, hybrid electric vehicles (HEV) and plug-in EV will become even more common in the near future [1]. The increased demand of energy by the EV will potentially put the operation of the distribution grid in a danger. Smart grid concepts for charging the EVs have been recently developed in [2]–[4] and many more that involve a mixture of renewable energy resources (mostly photovoltaic (PV)) and demand response.

The EV that are charged by single-phase chargers together with other single-phase loads will cause phase voltage difference between the three phase voltage hence, the voltage unbalance will be deteriorated. Furthermore, the majority of the distributed energy resources (DERs) is single-phase connected with a peak power between 1 to 5 kWp. It is well known that the DERs have positive impact over the grid performance if the produced energy meats the local demand. However, single-phase DERs in combination with single-phase charged EV might lead to even more prominent voltage unbalance problems if DERs and EVs are not connected to the same phase. This might lead to overvoltages due to the increased zero-sequence currents which will impose even more challenges to the distribution system operators (DSO) to maintain the power quality in their LV grids.

In [5], [6] a three-phase damping control strategy for three-phase DERs is proposed that is able to mitigate the voltage unbalance by emulating resistive behaviour towards the zero- and negative-sequence components. The proposed control strategy relies entirely on local measurements to mitigate the voltage unbalance and the necessity of a secondary control is avoided. In this article, the three-phase damping control strategy is modified to be able to supply a load and consumes power from the grid instead of injecting it. This control strategy can be used in charging poles or to charge EV that require a three-phase connection to the distribution grid. By modifying the three-phase damping control strategy to work in active rectifier mode, the voltage unbalance will be mitigated by drawing larger current from the phase with the highest voltage and smaller currents from the phases with the lower phase voltages. The classical control of the active rectifiers is usually implemented by drawing only positive-sequence current as studied in [7]. Therefore, a comparison between the classical positive-sequence and three-phase damping control strategies will be performed.

This article is organised as follows: In Section II, the analytical models of the used control strategies for active rectifiers are given and their practical implementation is described. In Section III, the experimental examinations are described and finally the conclusions are drawn.

II. Comparison between positive-sequence and damping control strategies

In this article, harmonic distortions will not be considered, and also further on, complex values (and thus only fundamental components) are used, thus

the p.u. value of the phase voltage $\underline{v}_x$ can be written in complex form as:

$$\underline{v}_x = |v_x| \exp(\mathrm{j}\theta_x) \tag{1}$$

with v_x the rms value of corresponding phase voltage $\underline{v}_x$, x is the phase of connection and θ_x is the corresponding phase angle.

A. Three-phase positive-sequence control strategy

One of the most common practice for controlling a three-phase active rectifier connected to the utility grid and having a unity power factor is done by drawing only positive-sequence current. This comes from the fact that most of the three-phase angle detection techniques are based on phase locked loop (PLL) algorithms that are using a synchronous reference frame [8]. In other words, the three-phase PLLs use a coordinate transformation from abc to dq and, therefore, the output signals of these PLLs have phase angles corresponding to the positive-sequence component of the grid voltage. If the phase angles are assumed to be:

$$\theta_a = 0, \theta_b = \theta_a - \frac{2\pi}{3}, \theta_c = \theta_a + \frac{2\pi}{3}$$

then the phase currents in the p.u. systems can be expressed as:

$$\underline{i}_{x,\mathrm{p}} = g_1 e^{(j\theta_x)} \tag{2}$$

where x represents the corresponding phase a, b or c and "p" denotes active power consumed by the load. The fundamental input conductance g_1 is written as:

$$g_{1,\mathrm{p}} = \frac{p^*_{\mathrm{dc}}}{3|\underline{v}_1|} \tag{3}$$

where p^*_{dc} is the requested power by the load and $\underline{v}_1$ is the rms value of the positive-sequence voltage. Obtaining the symmetrical components representation for the injected currents is done by the inverse Fortescue transformation which yields to the following symmetrical component equations:

$$\underline{i}_0 = 0, \underline{i}_1 = g_1 e^{(j\theta_1)}, \underline{i}_2 = 0 \tag{4}$$

where the indexes (*0,1,2*) are the zero-, positive-, and the negative-sequence components.

B. Three-phase damping control strategy

As mentioned above, the voltage unbalance is (or it will become in the future) one of the most common problem in LV grids with high penetration of DERs and EV. The three-phase damping control strategy is studied in [6], [9] and it is able to successfully mitigate the voltage unbalance at the point of common coupling (PCC). The idea behind the three-phase damping control strategy is as follows: the desired reaction of the three-phase damping control strategy is to behave resistively towards the zero- and negative-sequence voltage components in LV networks [5], [6]. The damping control strategy can be described mathematically by the following set of equations:

$$\begin{bmatrix} \underline{i}_0 \\ \underline{i}_1 \\ \underline{i}_2 \end{bmatrix} = \begin{bmatrix} g_d & 0 & 0 \\ 0 & g_1 & 0 \\ 0 & 0 & g_d \end{bmatrix} \begin{bmatrix} \underline{v}_0 \\ \underline{v}_1 \\ \underline{v}_2 \end{bmatrix} \tag{5}$$

where $\underline{v}_0$, $\underline{v}_1$ and $\underline{v}_2$ are the zero-, positive- and the negative-sequence voltage components, g_d is the fundamental damping conductance of the rectifier. Eq. (5) can be transformed into phase quantities by using:

$$\begin{bmatrix} \underline{i}_a \\ \underline{i}_b \\ \underline{i}_c \end{bmatrix} = T^{-1} \begin{bmatrix} g_d & 0 & 0 \\ 0 & g_1 & 0 \\ 0 & 0 & g_d \end{bmatrix} T \begin{bmatrix} \underline{v}_a \\ \underline{v}_b \\ \underline{v}_c \end{bmatrix} \tag{6}$$

where T is the transformation matrix from phase quantities (a, b, c) to symmetrical components (*0,1,2*). Consequently, the following equations for the phase currents are obtained:

$$\begin{aligned} &\underline{i}_a = \\ &\frac{1}{3}\{\underline{v}_a(g_1 + 2g_d) + a\underline{v}_b(g_1 - g_d) + a^2\underline{v}_c(g_1 - g_d)\} \\ &\underline{i}_b = \\ &\frac{1}{3}\{a^2\underline{v}_a(g_1 - g_d) + \underline{v}_b(g_1 + 2g_d) + a\underline{v}_c(g_1 - g_d)\} \\ &\underline{i}_c = \\ &\frac{1}{3}\{a\underline{v}_a(g_1 - g_d) + a^2\underline{v}_b(g_1 - g_d) + \underline{v}_c(g_1 + 2g_d)\} \end{aligned} \tag{7}$$

with $a = e^{\mathrm{j}2\pi/3}$. If (1) is substituted in (7), the following equations for the phase currents are obtained:

$$\begin{aligned}
\underline{i}_a &= \frac{1}{3}\Bigg\{ g_1 \left[|v_a| e^{\mathrm{j}\theta_a} + |v_b| e^{\mathrm{j}(\theta_b + \frac{2\pi}{3})} + |v_c| e^{\mathrm{j}(\theta_c - \frac{2\pi}{3})} \right] \\
&\quad + g_d \left[2|v_a| e^{\mathrm{j}\theta_a} - |v_b| e^{\mathrm{j}(\theta_b + \frac{2\pi}{3})} - |v_c| e^{\mathrm{j}(\theta_c - \frac{2\pi}{3})} \right] \Bigg\} \\
\underline{i}_b &= \frac{1}{3}\Bigg\{ g_1 \left[|v_b| e^{\mathrm{j}\theta_b} + |v_a| e^{\mathrm{j}(\theta_a - \frac{2\pi}{3})} + |v_c| e^{\mathrm{j}(\theta_c + \frac{2\pi}{3})} \right] \\
&\quad + g_d \left[2|v_b| e^{\mathrm{j}\theta_b} - |v_a| e^{\mathrm{j}(\theta_a - \frac{2\pi}{3})} - |v_c| e^{\mathrm{j}(\theta_c + \frac{2\pi}{3})} \right] \Bigg\} \\
\underline{i}_c &= \frac{1}{3}\Bigg\{ g_1 \left[|v_c| e^{\mathrm{j}\theta_c} + |v_a| e^{\mathrm{j}(\theta_a + \frac{2\pi}{3})} + |v_b| e^{\mathrm{j}(\theta_b - \frac{2\pi}{3})} \right] \\
&\quad + g_d \left[2|v_c| e^{\mathrm{j}\theta_c} - |v_a| e^{\mathrm{j}(\theta_a + \frac{2\pi}{3})} - |v_b| e^{\mathrm{j}(\theta_b - \frac{2\pi}{3})} \right] \Bigg\}
\end{aligned} \tag{8}$$

where terms in (8) related to g_1 can be interpreted as the steady-state value of the fundamental component of the drawn current. These terms are adapted by the dc-bus voltage controller in order to balance the power exchanged with the grid. Since the dc-bus voltage controller is slow, g_1 is slowly varying. The terms related to g_d emulate the resistive behaviour towards the zero- and negative-sequence voltage components.

In practice, the power balance between the dc side and the utility grid is maintained by using a dc-bus controller, the output of which is the fundamental conductance g_1 of the power electronic rectifier [10]. In order to incorporate the input conductance into a simulation model, the following equation can be used:

$$\begin{aligned}
g_1 &= \frac{3\ p^*_{\mathrm{dc}}}{\sum |\underline{v}_x|^2 + 2\ \sum_{x \neq y} |v_x||v_y| \cos(\theta_{\mathrm{x}} - \theta_{\mathrm{y}} - \frac{2\pi}{3})} \\
&\quad - 2 g_d \frac{\sum |\underline{v}_x|^2 - \sum_{x \neq y} |v_x||v_y| \cos(\theta_{\mathrm{x}} - \theta_{\mathrm{y}} - \frac{2\pi}{3})}{\sum |\underline{v}_x|^2 + 2\ \sum_{x \neq y} |v_x||v_y| \cos(\theta_{\mathrm{x}} - \theta_{\mathrm{y}} - \frac{2\pi}{3})}
\end{aligned} \tag{9}$$

The term of the positive-sequence fraction describes the exchanged active power with the grid and the term determined by the second fraction compensates for the power of the zero-sequence and the negative-sequence components [9]. This control strategy mitigates the voltage unbalance by drawing lower current in the phase with lower voltage and higher current in the phase with higher voltage. The damping capabilities of this control strategy are determined by the damping conductance g_d which can be calculated by using the nominal ratings of the power electronic rectifier:

$$G_d = \frac{P_{\mathrm{DC_{nom}}}}{V^2_{\mathrm{nom}}} \tag{10}$$

where $P_{\mathrm{DC_{nom}}}$ is the nominal power of the rectifier and V_{nom} is the nominal value of the grid voltage. In a p.u. system the damping conductance is expressed as:

$$g_d = \frac{P_{\mathrm{nom}}/P_{\mathrm{DC_{base}}}}{V^2_{\mathrm{nom}}/V^2_{\mathrm{base}}} \tag{11}$$

where P_{base} is the base power of the power electronic rectifier and V_{base} is the base value of the grid voltage. In [5], [6], [9], the three-phase damping control strategy is studied when used in renewable energy applications. In this mode, the fundamental input conductance has a negative sigh and the damping conductance has a positive sign. When the three-phase damping control strategy is used as an active rectifier, the fundamental input conductance has a positive sign and the damping conductance has a positive sign, too.

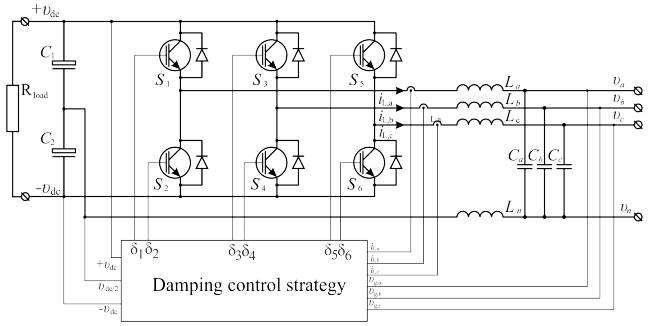

Fig. 1. Three-phase four-wire inverter used by the three-phase damping control strategy

C. Practical implementation

In order to react on the zero-sequence voltage component, the three-phase damping control strategy requires a three-phase four-wire inverter. The inverter topology uses a split dc-bus capacitor to form the neutral connection as shown in Fig. 1. The voltage equilibrium is maintained by using two dc-bus controllers for each capacitor C_1 and C_2 as implemented in [11].

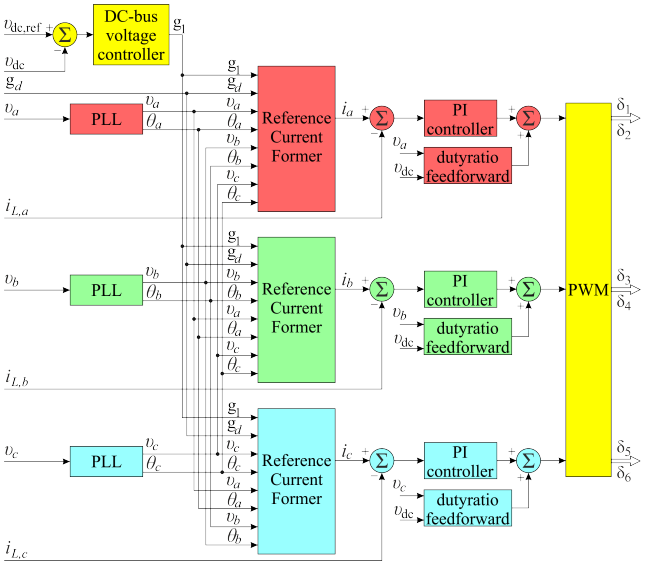

Fig. 2. Block diagram of the practical implementation of the three-phase damping control strategy

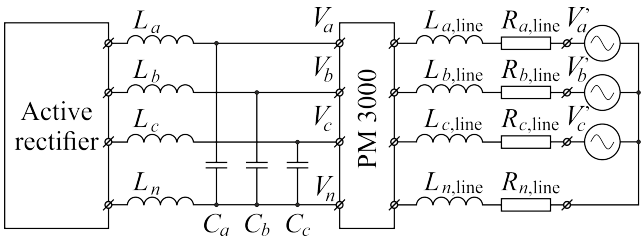

Fig. 3. Connection diagram of the experimental set-up

The power electronic switches are driven by a digital signal processor TMS320F28335 in which the three-phase positive-sequence and damping control strategies are implemented. A simplified block diagram of the three-phase damping control strategy is depicted in Fig. 2. The magnitudes and the angles of the phase voltages at the rectifier terminals are extracted by using three PLL blocks. These signals together with the fundamental input and damping conductances are passed to the reference current former block in which (8) is used to calculate the reference currents. The reference and measured currents are subtracted and the error is fed to a PI controller. Since the PI controller has poor reference tracking to sinusoidal signals an additional duty ratio feed forward compensation is included and the resultant signal is passed to a PWM former that generates the driving sequence for the power electronic switches.

TABLE I
TEST SET-UP PARAMETERS

Parameter	Value
V_a',V_b' and V_c'	117 V, 106 V, 106 V (50 Hz)
$Z_{a,\text{line}}$, $Z_{b,\text{line}}$, $Z_{c,\text{line}}$, and $Z_{n,\text{line}}$	(0.470+j0.201)
Power analyser	PM3000
C_a, C_b and C_c	5 μF
L_a, L_b and L_c	2 mH
L_n	0.666 mH
Load power	0.8 kW
C_1 and C_2	2000 μF
$V_{\text{dc,p}}$+$V_{\text{dc,n}}$	400 V
Switching frequency	20 kHz
Current base value	7.5 A
Phase voltage base value	225 V
dc-bus voltage base value	200 V

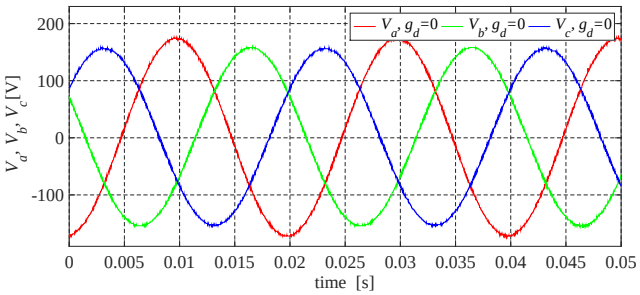

Fig. 4. Phase voltage measured at the rectifier terminals

III. Experimental Results

The experimental validation of the proposed active rectification control is performed by using a set-up that is presented in Fig. 3. The three-phase four-wire rectifier is connected to a three-phase programmable voltage source via a power analyser and a cable. More information about the set-up parameters can be found in Table I. The programmable voltage source is able to deliver asymmetrical voltages V_a',V_b' and V_c' which will force the three-phase damping control strategy to draw asymmetrical currents. The control strategies are implemented in the p.u. system because the transition from power flow simulation platforms to practical implementation is done in a more easy way. However, the experimental results are presented in absolute values which will give more useful information about the exchanged currents by the different control strategies and also the performance assessment can be done easily.

The instantaneous phase voltages at the rectifier terminals are measured by using an oscilloscope and a Matlab script to depict the measurements which are shown in Fig. 4. In Fig. 5 are presented the phase currents when the damping conductance $g_d =$

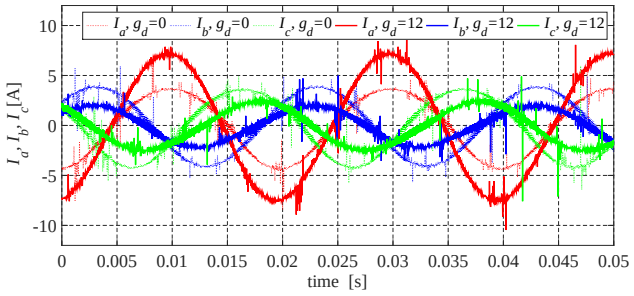

Fig. 5. Phase currents drawn by the three-phase damping control strategy

0 p.u. and 12 p.u. When $g_d = 0$ p.u. this corresponds to the positive-sequence control strategy thus, only positive-sequence current is been drawn from the voltage source. Therefore, the zero- and negative-sequence remain intact. On the other hand, when the $g_d = 12$ p.u. the drawn phase currents are not equal in magnitude any more. The damping control strategy draws more current from phase a where the phase voltage is the highest compared to phases b and c and draws lower currents from phases b and c. Thus, the voltage unbalance at the PCC is mitigated.

From (8) it can be seen that besides the current magnitudes, the phase currents will also have a change in the phase angles which is also dependent on the g_d value. In Table II additional data are listed when different values of the damping conductance are used. The experimental results show that the phase currents experience some small change in the phase angles which leads to some reactive power flow. Despite the non unity power factor, the damping control strategy is based on the symmetrical component theory and this reactive power flow helps to reduce the voltage unbalance in a natural way without causing additional feeder losses.

According to standard EN50160 [12], the negative-sequence voltage unbalance factor (VUF) is calculated as a ratio between the negative-sequence and positive-sequence voltage components:

$$\mathrm{VUF}_2 = \frac{V_2}{V_1}.100[\%] \tag{12}$$

Standard [12] does not set any limits on the zero-sequence voltage unbalance factor but [5], [6] report that the zero-sequence component has a direct impact on the overvoltages hence, VUF_0 is also examined. In Fig. 6 are depicted the different values of

TABLE II
VOLTAGES AND CURRENTS MEASURED AT THE INVERTER TERMINALS

	$\underline{V}_a$	$\underline{V}_b$	$\underline{V}_c$
$g_d = 0$ [p.u.]	115.9V $\angle 0°$	105.0V $\angle 120.3°$	104.9V $\angle 240.2°$
$g_d = 1$ [p.u.]	115.6V $\angle 0°$	105.1V $\angle 120.3°$	105.1V $\angle 240.1°$
$g_d = 5$ [p.u.]	114.6V $\angle 0°$	105.7V $\angle 120.5°$	105.6V $\angle 239.8°$
$g_d = 8$ [p.u.]	114.1V $\angle 0°$	106.0V $\angle 120.6°$	105.9V $\angle 239.7°$
$g_d = 12$[p.u.]	113.5V $\angle 0°$	106.3V $\angle 120.7°$	106.2V $\angle 239.6°$
	$\underline{I}_a$	$\underline{I}_b$	$\underline{I}_c$
$g_d = 0$ [p.u.]	2.688A $\angle 5.7°$	2.620A $\angle 125.6°$	2.612A $\angle 245.6°$
$g_d = 1$ [p.u.]	2.906A $\angle 5.2°$	2.493A $\angle 126.1°$	2.484A $\angle 245.8°$
$g_d = 5$ [p.u.]	3.810A $\angle 3.7°$	2.021A $\angle 131.0°$	1.976A $\angle 243.9°$
$g_d = 8$ [p.u.]	4.325A $\angle 3.1°$	1.803A $\angle 137.2°$	1.686A $\angle 240.0°$
$g_d = 12$ [p.u.]	4.930A $\angle 2.7°$	1.571A $\angle 147.1°$	1.380A $\angle 231.8°$

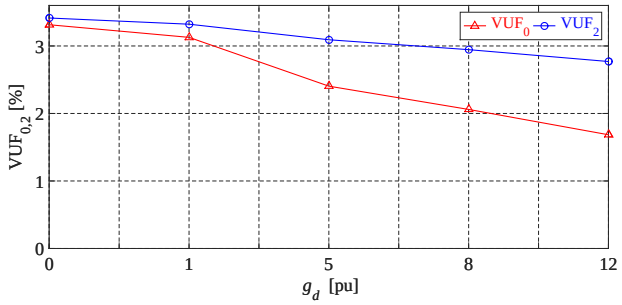

Fig. 6. Zero-, and negative-sequence voltage unbalance factors at the PCC

the zero- and negative-sequence voltage unbalance factors when different values of g_d are used where VUF_0 is calculated in the same manner as 12. It can be clearly seen that when the damping conductance differs from zero the values of the VUF_0 and VUF_2 are decreased, especially when $g_d \geq 5$ p.u.

IV. Conclusion

In this article, the three-phase damping control strategy is examined in an active rectifier mode and the experimental results showed that the control strategy will draw more current(s) from the phase(s) with the higher voltage and less current will be drawn from the phases with the lower voltage(s). Thus the voltage unbalance will be mitigated. This makes the three-phase damping control strategy very attractive for integration in devices that require three-phase active rectifiers such as motor drives and battery chargers and it can successfully substitute the power factor correctors which are currently used in these devises.

Acknowledgment

This work is supported by EC-FP7 project INCREASE with Grant agreement: 608998.

REFERENCES

[1] H. R. Galiveeti, A. K. Goswami, and N. B. D. Choudhury, "Impact of plug-in electric vehicles and distributed generation on reliability of distribution systems," *Engineering Science and Technology, an International Journal*, vol. 21, no. 1, pp. 50 – 59, 2018.

[2] K. N. Kumar and K. J. Tseng, "Impact of demand response management on chargeability of electric vehicles," *Energy*, vol. 111, pp. 190 – 196, 2016.

[3] J. W. Eising, T. van Onna, and F. Alkemade, "Towards smart grids: Identifying the risks that arise from the integration of energy and transport supply chains," *Applied Energy*, vol. 123, pp. 448 – 455, 2014.

[4] N. Nezamoddini and Y. Wang, "Risk management and participation planning of electric vehicles in smart grids for demand response," *Energy*, vol. 116, pp. 836 – 850, 2016.

[5] D. Bozalakov, T. Vandoorn, B. Meersman, C. Demoulias, and L. Vandevelde, "Voltage dip mitigation capabilities of three-phase damping control strategy," *Electric Power Systems Research*, vol. 121, pp. 192 – 199, 2015.

[6] D. V. Bozalakov, T. L. Vandoorn, B. Meersman, G. K. Papagiannis, A. I. Chrysochos, and L. Vandevelde, "Damping-based droop control strategy allowing an increased penetration of renewable energy resources in low-voltage grids," *IEEE Transactions on Power Delivery*, vol. 31, no. 4, pp. 1447–1455, Aug 2016.

[7] H. Tanaka, F. Ikeda, T. Tanaka, H. Yamada, and M. Okamoto, "Novel reactive power control strategy based on constant dc-capacitor voltage control for reducing the capacity of smart charger for electric vehicles on single-phase three-wire distribution feeders," *IEEE Journal of Emerging and Selected Topics in Power Electronics*, vol. 4, no. 2, pp. 481–488, June 2016.

[8] F. Blaabjerg, R. Teodorescu, M. Liserre, and A. V. Timbus, "Overview of control and grid synchronization for distributed power generation systems," *IEEE Transactions on Industrial Electronics*, vol. 53, no. 5, pp. 1398–1409, Oct 2006.

[9] B. Meersman, B. Renders, L. Degroote, T. Vandoorn, and L. Vandevelde, "Three-phase inverter-connected dg-units and voltage unbalance," *Electric Power Systems Research*, vol. 81, no. 4, pp. 899 – 906, 2011.

[10] T. L. Vandoorn, B. Meersman, L. Degroote, B. Renders, and L. Vandevelde, "A control strategy for islanded microgrids with dc-link voltage control," *IEEE Transactions on Power Delivery*, vol. 26, no. 2, pp. 703–713, April 2011.

[11] D. Bozalakov, B. Meersman, A. Bottenberg, J. Rens, J. Desmet, and L. Vandevelde, "Dc-bus voltage balancing controllers for split dc-link four-wire inverters and their impact on the quality of the injected currents," *CIRED - Open Access Proceedings Journal*, vol. 2017, no. 1, pp. 564–568, 2017.

[12] "Voltage characteristics of electricity supplied by public distribution networks," *EN Standard 50160-2008*, 2008.